1    Corollary discharge prevents signal distortion and enhances sensing during locomotion

2

3    Dimitri A. Skandalis*,†, Elias T. Lunsford, James C. Liao*

4    Department of Biology & Whitney Laboratory for Marine Bioscience, University of
5    Florida

6    † Current address: Department of Psychological & Brain Sciences, Johns Hopkins
7    University

8

9    * Correspondence: da.skandalis@gmail.com, jliao@whitney.ufl.edu

10

11    DAS ORCID: 0000-0002-5126-958

12

13    **Classification**

14    Biological Sciences, Neuroscience

15    **Keywords – 3 to 5**

16    Efference copy; hair cells; flow sensing; signal processing; sensorimotor integration

17    **Author Contributions**

18    DAS, ETL, and JCL conceived experiments; DAS and JCL designed experiments; DAS
19    performed experiments and analyzed results; DAS wrote the manuscript; DAS, ETL, and
20    JCL edited the manuscript. Resources: JCL; Project administration: JCL; Funding
21    acquisition: JCL. All authors approved the manuscript in its final form.

22

23

24    **This PDF file includes:**
25    Main Text
26    Figures 1 to 5

**Abstract**

Sensory feedback during movement entails sensing a mix of externally- and self-generated stimuli (respectively, exafference and reafference). In many peripheral sensory systems, a parallel copy of the motor command, a corollary discharge, is thought to eliminate sensory feedback during behaviors. However, reafference has important roles in motor control, because it provides real-time feedback on the animal's motions through the environment. In this case, the corollary discharge must be calibrated to enable feedback while avoiding negative consequences like sensor fatigue. The undulatory motions of fishes' bodies generate induced flows that are sensed by the lateral line sensory organ, and prior work has shown these reafferent signals contribute to the regulation of swimming kinematics. Corollary discharge to the lateral line reduces the gain for reafference, but cannot eliminate it altogether. We develop a data-driven model integrating swimming biomechanics, hair cell physiology, and corollary discharge to understand how sensory modulation is calibrated during locomotion in larval zebrafish. In the absence of corollary discharge, lateral line afferent units exhibit the highly heterogeneous habituation rates characteristic of hair cell systems, typified by decaying sensitivity and phase distortions with respect to an input stimulus. Activation of the corollary discharge prevents habituation, reduces response heterogeneity, and regulates response phases in a narrow interval around the time of the peak stimulus. This suggests a synergistic interaction between the corollary discharge and the polarization of lateral line sensors, which sharpens sensitivity along their preferred axes. Our integrative model reveals a vital role of corollary discharge for ensuring precise feedback, including proprioception, during undulatory locomotion.

51 **Main Text**
52
53 **Introduction**
54  While moving through the environment, animals detect a mix of sensory signals

55 originating from external sources and from the animal itself. Sensors provide feedback

56 from the environment (exafference), but because they are embedded in a body moving

57 through the environment, self-stimulation (reafference) is unavoidable. Reafference has

58 commonly been considered a sensory artefact that interferes with appropriate behavior

59 selection. For example, vigorous reafference could be mistaken for an impending attack,

60 leading to the inappropriate activation of reflexive escape circuits (1, 2). Sustained

61 reafference also fatigues sensors, reducing sensitivity and distorting the timing of neural

62 signals (3, 4); in the extreme, overstimulated sensory circuitry may lead to excitotoxic

63 cell death (5). For these reasons, many sensory pathways are modulated by feedforward

64 neural signals activated in parallel with motor circuitry, which decrease sensor gain or

65 eliminate reafferent signals altogether. These pathways, called corollary discharge (CD),

66 mitigate negative consequences of reafference (1, 6). Well-studied examples of CD

67 include the activities of inhibitory interneurons in crickets, crayfish, and tadpoles, which

68 silence sensory circuitry during motor bouts (1, 2, 7, 8). This silencing is costly if it

69 causes the organism to miss salient events in the environment. However, by focusing on

70 sensing exafference and eliminating reafference, the field has tended to overlook the

71 critical role of reafference in adaptive behavior and the negative consequences of

72 suppressing reafference. Although reafference may entail negative consequences in terms

73 of sensory ambiguity and sensor fatigue, it is nonetheless the error signal on which motor

74 learning and sensor planning are based (1, 9–11). Reafference encodes crucial

75 information about the animal's own body parts with respect to the environment, such as

76 relative orientation, speed, and acceleration (12–14). A key question of sensorimotor

77 integration is therefore how CD can contribute to the regulation of the negative and

78 positive aspects of reafference in light of behavioral demands.

79  The fish lateral line system is essential for informing behaviors such as schooling,

80 prey detection, and rheotaxis (12, 15–18). The lateral line transduces fluid motions within

81 the boundary layer through the bending of neuromast cupulae, depolarization of hair

82    cells, and ultimately the transmission to the brain of afferent fiber spike activity (19–23).

83    Because of this arrangement, the lateral line system is naturally subject to large amounts

84    of reafference during undulatory swimming motions (23–25) (Figure 1 A). Fish have

85    been found to rely on reafference signaling to provide proprioceptive feedback for

86    swimming kinematics, though its mechanisms remain poorly understood [reviewed in

87    (23, 24)]. The dependence on reafference becomes most evident at higher swim speeds

88    and in turbulent flow conditions, in which cases the loss of lateral line feedback leads to

89    progressively diverging kinematics (24, 26). It remains unclear what lateral line signals

90    could provide proprioceptive feedback. Here, we reasoned that because the mechanical

91    body wave (Figure 1 A) is consistently dysregulated by lateral line ablation (24, 26),

92    sensing of the body wave itself is a component of proprioception. To understand how

93    feedback from the lateral line thus contributes to kinematic control, we propose a model

94    integrating the biomechanics of axial undulation (Figure 1 A) with lateral line neuromast

95    biophysics. Axial undulations are fundamental to fish locomotion and are robustly

96    transduced through periodic spiking in the lateral line (23–25, 27). The position of the

97    peak of the body wave can therefore be inferred from the phase lag between the

98    maximum spike rates of afferent fibers innervating sequential neuromasts (maximum

99    cupular deflection, Figure 1 Aii,iii). As we show here, modulation of hair cell gain by the

100   CD is a key component of the lateral line circuit that allows the fish to maintain a faithful

101   representation of the body wave position.

102   　　　　Hair cell physiology could be expected to limit the accuracy of sensory feedback

103   during continuous stimulation. Hair cell systems, including the lateral line, exhibit high

104   stimulus gain (nanometer accuracy, (28)) combined with finite vesicle populations (29,

105   30). Protracted stimulation, as occurs during locomotion, results in rapidly depressing

106   responses, known as synaptic depression or habituation (21, 31–33), which can result in

107   distortions of signal response phase, including delayed or advanced spike timings (3, 32).

108   We illustrate this in Figure 1 Bii by comparing the spike phase distribution of an

109   idealized sensor to that of a habituating sensor. The output of the idealized sensor is

110   strictly proportional to cupular deflection along its axis of polarized sensitivity (34). The

111   proportionality dictates that peak sensory feedback coincides with the maximum cupula

112    deflection, which is taken to be at a stimulus phase of $\pi/2$ for our sinusoidal kinematic

113    approximation. The median afferent fiber spike phase therefore serves as a detector of the

114    peak of the body wave, and the phase lag between sequential neuromasts would mark its

115    antero-caudal progression (Figure 1 A iii, B). Under the parameters of this model, a

116    distortion of spike phase responses will impact the ability to accurately sense the body

117    wave and coordinate kinematics. Synaptic depression leads to phase-advanced responses

118    within a stimulus cycle (relative to the stimulus phase) and phase-delayed responses from

119    the first to the last stimulus cycles [Figure 1 B, predictions based on (21, 32, 33)]. Further

120    convoluting these distortions is the fact that lateral line habituation rates are highly

121    variable, differing even among hair cells within a single neuromast (21). Heterogeneous

122    habituation rates are expected to cause divergent afferent fiber signals over the course of

123    the swim bout, complicating the task of tracking the timing of the body wave. Controlling

124    heterogeneous gain within the lateral line should be of paramount importance in

125    accurately sensing the position of the traveling body wave while swimming.

126          The CD to the lateral line tonically modulates the sensitivity of the lateral line

127    during swim bouts (25, 35–37). Efferent projections from the hindbrain synapse on hair

128    cells and evoke an inhibitory hyperpolarizing current while swimming, reducing the

129    amount of presynaptic glutamate vesicle release (38–40). Hyperpolarization increases the

130    current required to evoke exocytosis, which demands a larger cupular deflection to

131    achieve the same afferent fiber activity. In addition to the reduced number of spontaneous

132    and evoked afferent fiber spikes (25, 37, 40), the higher deflection threshold will also

133    narrow the response interval (which in turn increases vector strength, Figure 1 Bii). The

134    narrower interval results from delayed early spikes and advanced late spikes (as measured

135    by the quantiles of the spike phase distribution), and affects sustained responses in two

136    important ways. First, the propensity for habituation is reduced as the response interval

137    narrows, because fewer vesicles are expected to be released (i.e., afferent activity is

138    reduced). Second, preventing habituation will maintain afferent fiber spikes that are well-

139    timed with respect to self-stimulation, and therefore can have proprioceptive functions.

140    As the deflection threshold increases, it will eventually be equal only to the largest

141    depolarization experienced by the hair cells in one neuromast, meaning that all afferent

5

142   fiber activity will be concentrated on a single time point. We propose that this point is the

143   maximum deflection of the cupula, which corresponds to the passing of the peak of the

144   body wave (Figure 1 Aii). In this way, the self-stimulated afferent fiber activity signals

145   peak body bending.

146        Because the lateral line sensors are so heterogeneous, how they are affected by

147   CD may also be highly heterogeneous (41). This heterogeneity prompted us to study the

148   role of CD on lateral line dynamics with three goals in mind. First, we use

149   electrophysiology to detail among-unit differences in the magnitudes of habituation and

150   CD on evoked spike rates. Second, we study afferent fiber responses, including spike rate

151   and phase, when the CD is OFF (fish is inactive) or ON (fish is swimming). Finally, we

152   simulate afferent fiber responses during CD OFF and ON to examine the lateral line's

153   capacity to accurately signal the timing of peak stimulation by the passing body wave.

154   Our results are consistent with the hypothesis that CD to the fish lateral line evolved to

155   precisely control hair cell gain while swimming and pass spikes that convey useful

156   proprioceptive information.

157   **Results**
158   *Interactions between habituation and corollary discharge affect spike rate and timing*

159        The role of corollary discharge (CD) in regulating lateral line responses while

160   swimming was examined in larval zebrafish (*Danio rerio*). Swimming activity was

161   identified in immobilized larvae using extracellular recordings from ventral motor nerve

162   roots, while lateral line activity was determined from patch clamp recordings (loose-patch

163   configuration) of single afferent neurons (hereafter referred to as units) in the posterior

164   lateral line afferent ganglion. Single neuromasts were sinusoidally stimulated using a

165   glass bead affixed to a piezoelectric transducer at 5, 20, or 40 Hz to simulate the normal

166   tail beat frequencies of freely swimming larvae (37, 42). Afferent fiber responses rapidly

167   habituated to stimulation (exemplar trace at 20 Hz and peristimulus time histogram

168   (PSTH), Figure 1 Ai, ii; 5 and 40 Hz in Supplementary Fig. S1; see also (21, 33)). The

169   rapid decay followed by a refractory period (Figure 2 Aii) is similar to recordings in other

170   recordings from lateral line and auditory afferent fibers (30, 33, 43). Responses to the

6

171     first stimulus ranged from 1.2 – 5.4× that of the last stimulus. On average, the change in

172     spontaneous and evoked spike rates (ΔS and ΔE, respectively) during swim periods

173     (when the CD is active, CD ON) ~50% of inactive period (CD OFF; $p<0.001$,

174     Supplementary Fig. S2; 5859 total swims), comparable to previous measurements (37,

175     40). However, the joint distribution of ΔS and ΔE revealed significant differences in

176     some cells of the effects of CD on spontaneous and evoked spike rates (Figure 2 B *i*). We

177     found that this was due to an interaction between the level of observed suppression and

178     level of habituation (habituation = first-last response; ΔS × habituation: $p=0.01$, CI: -

179     0.54– -0.08). We therefore applied cluster analysis based on ΔS, ΔE, and habituation

180     level to identify characteristics of different groups of responses among lateral line

181     afferent units (Figure 2 B *i*). Four identified groups corresponded to each permutation of

182     low and high levels of inhibition strength and degree of habituation, as verified by post-

183     hoc analysis (Figure 2 B *ii,iii*).

184             The differences among groups suggested that interactions between habituation

185     and CD identify a significant source of heterogeneity within and among afferent fibers

186     during swim bouts. In order to understand how this heterogeneity could impact

187     reafference signalling in our model (Figure 1), we next examined the dynamics of

188     afferent spike count and phase in response to stimulation during CD OFF (black in Figure

189     3). The PSTHs reveal substantial phase distortions from the first to last stimulus intervals

190     at each frequency (Figure 3 A). In parallel to the decline of spike count, the phase

191     distortions resulted in narrower response intervals over time, and therefore increased

192     vector strength (Figures 3 Bi, Ci; quantified through generalized additive models, GAM).

193     The inverse relationship between spike count and vector strength was likewise observed

194     among the four cell groups, such that Groups 1 and 2 exhibited lower average spike

195     counts and vector strengths compared to Groups 3 and 4. To quantify time-dependent

196     changes in lateral line sensitivity, we calculated afferent fiber gain (20) as the product of

197     spike count and vector strength. Based on this measure, we suggest that cells in Groups 1

198     and 2 cells have low gain (average gain <1) whereas units in Groups 3 and 4 cells have

199     high gain (gain >1; Figure 3 Ciii). Average and group-specific gain strongly declined due

200     to habituation (Figure 3 Biii). The gain of units in Groups 1 and 2 was slightly greater

201   than unity for initial stimuli, but fell to substantially less than unity subsequently. Units in

202   Groups 3 and 4 maintained gain ≥1 but with very large relative changes (Figure 3 Biii).

203   The PSTHs also suggested that habituation more substantially delayed the timing of the

204   earliest spikes (spike latency) than of later spikes. We corrected for the frequency-

205   dependent phase shift caused by linear conduction delays in the afferent fibers (20) by

206   subtracting each unit's median phase at each frequency. All quantiles of the spike phase

207   distribution were delayed, indicating that the response interval is shifted as well as being

208   narrowed (as indicated by vector strength). Average responses among groups coincided

209   with the differences in vector strength, such that cells in Groups 3 and 4 had much

210   narrower response distributions (Figure 3C iv).

211        Average responses varied widely across frequencies. Spike count and vector

212   strength were inversely related, respectively decreasing and increasing at higher

213   frequencies, resulting in a decline in per-stimulus gain to less than unity (Figure 3 Di-iii).

214   The narrower response intervals are reflected in the response phases (Figure 3 Div).

215   Because average responses varied widely, we expressed the effect of habituation as the

216   difference between the first and last stimulus intervals relative to the average CD OFF

217   response (Δ% in Figure 3). The effect of habituation was not explicitly parametrized in

218   our models, so was calculated from samples drawn from the model posterior distributions

219   (the smooth functions are nonparametric). Habituation had a small effect on spike count

220   and gain at 5 Hz compared to 20 and 40 Hz (Figures 2 Bii, Cii). There was no statistically

221   distinguishable effect on vector strength across frequencies, which also all overlapped

222   zero. However, response phase was significantly delayed at 20 and 40 Hz, but not at 5 Hz

223   (Figure 2 Div). Moreover, the phase of early spikes was more affected than that of late

224   spikes; for example, at 20 Hz, $0.1q$ and $0.5q$ phase were delayed by $0.48\pi$ (CI: 0.23–0.73)

225   and $0.44\pi$ (CI: 0.36–0.51), whereas $0.9q$ was 0.28 (CI: 0.04–0.39). This asymmetry

226   implies a narrower response interval which, as noted, was only weakly supported by the

227   vector strength measurement. This could be due to differences in calculation and

228   statistical power between the two measurements; vector strength is calculated from all

229   spikes, including outliers that fall outside the preferred phase (which can be seen in e.g.,

230    Figure 2A). The use of quantiles eliminates these outliers, which we suggest helps to

231    identify consistent changes despite the highly variable effects of habituation.

232           We next sought to quantify the average effects of CD ON. The relative difference

233    between CD OFF and CD ON was modelled as an intercept shift between the average

234    responses in each condition, expressed relative to CD OFF ($\Delta$CD% in Figure 3). Across

235    all frequencies, CD ON decreased spike count and increased vector strength, including at

236    5 Hz despite the negligible effects of habituation. This is superficially similar to

237    habituation, but in contrast to habituation, CD delayed early spike phases but advanced

238    late spikes' phase (Figure 3 Div). In this case, the asymmetric change in response

239    intervals implied by the spike phase quantiles was supported by the vector strength,

240    particularly at 5 Hz. We interpret these results to indicate that both habituation and CD

241    OFF decrease sensors' gain for the stimulus, which progressively reduces lateral line

242    sensitivity to all but the cupular peak deflection (stimulus phase of $\pi/2$). Thus the effect

243    of intense habituation, like CD ON, should be to create a more faithful representation of

244    the body wave, as implied by our model in Figure 1. However, the change in gain due to

245    habituation will depend on highly variable intercellular differences (Figure 2 B,C) as well

246    as variable effects of motor frequency and duration (see also, (37, 42)). Thus, habituation

247    should be an intrinsically unreliable mechanism for increasing the fidelity of afferent

248    responses with respect to the input stimulus. It is also noteworthy that the responses to

249    habituation and CD were more similar at 20 and 40 Hz than 5 Hz. We suggest that this is

250    because 5 Hz stimulation lies below typical larval tail beat frequencies (37, 42), and

251    therefore levels of habituation, to which the CD is adapted.

252    *Tuning hair cell gain prevents habituation and maximizes post-swim sensitivity*.

253           Our recordings suggested that CD can prevent habituation to maintain sensitivity

254    to post-swim stimuli. We typically observed an immediate restoration of sustained

255    evoked spike rates when a swim bout ended during a stimulus interval (Figure 2 A), or

256    even bursts of evoked spikes otherwise only seen at the start of the stimulus presentation

257    (examples highlighted in Supplementary Fig. S1). Swim-timing dependent responses in

258    spike rate and phase are obscured by our open-loop experimental setup and subsequent

9

259     analyses (Figure 2) in which we averaged over evoked responses occurring at different

260     relative times within distinct swim bouts. Thus, we normalised all swim bouts and an

261     equal post swim period to unit duration and then analysed response properties (spike rate,

262     vector strength, gain, and spike phase quantiles) of swims falling entirely within or

263     outside the stimulus period. This allowed us to quantitatively address the role of CD

264     during and after swim bouts, and our prediction that CD preserves constant phase

265     response.

266           Afferent unit responses during and after swim bouts substantially differed from

267     responses over the course of habituation. In contrast to the decline in spike count due to

268     habituation, evoked spike counts increased nearly linearly over the swim duration

269     (significance of smooth, $p<0.001$, Figure 4 A). Whereas spike activity was depressed

270     after the stimulus period with CD OFF (Figure 2 A *ii*), spike activity after the swim bout

271     actually peaked. The time course of spontaneous spike rate likewise exhibited a post-

272     swim peak ($p<0.001$; Figure 4 A), which is consistent with the effect of electrical

273     stimulation of inhibitory efferent fibers that causes vesicle accumulation and then post-

274     inhibition rebound activity (38). The increase in spontaneous spike rate and evoked spike

275     count over time can therefore be traced to the increasing cumulative probability of release

276     over time due to vesicle accumulation (38). That it occurs during stimulation points to the

277     CD protecting the vesicle pool from evoked release, given the level of stimulus that we

278     applied.

279           We predicted that CD ON would maintain a constant response interval and

280     median spike phase from the first to last stimulus periods (Figure 1 Bii). Instead, vector

281     strength somewhat decline over the course of the swim ($p=0.005$), reaching a post-swim

282     minimum coinciding with the timing of the evoked spike count maximum (Figure 4 B).

283     The regulation of spike rate and interval width by CD resulted in maximum gain (spike

284     count × vector strength) for stimuli in the post-swim period (Figure 4 C), indicating a

285     preservation to respond to post-swim stimuli. The changes in response interval over time

286     were due to continuous changes in the timing of both the earliest and latest spikes. With

287     CD ON, the response interval was narrow due to delayed $0.1q$ and advanced $0.9q$,

288    relative to the post-swim phase with CD OFF ($0.1q$: $p$=0.02: $0.9q$, $p$=0.008). Although

289    the phase quantile dynamics were asymmetrical, an essentially constant median spike

290    phase ($p$=0.31, Figure 4 D) was preserved throughout.

291    *Corollary discharge prevents phase distortion due to habituation*

292    　　　　Our results indicated that variation in gain is fundamental to understanding

293    heterogeneity within the lateral line, and thus the impact of CD on sensing. We developed

294    a computational simulation of afferent fiber responses to further probe the interactions

295    between heterogeneity in afferent fiber gain, CD strength, and afferent fiber response

296    phase. Our simulation is based on a conceptual model of vesicle pool depletion (CD

297    OFF) or conservation (CD ON). Simulated vesicles transitioned between four states:

298    bound and ready for release; releasing, which was taken as a spike; released and

299    unavailable for signaling; or regenerating by returning to the ready state (Figure 5B *i*).

300    Simulated fibers recapitulated the time-averaged features of the CD OFF condition,

301    namely a strong response to the first stimulus, a habituated response to subsequent

302    stimuli, a refractory period after stimulation, and variable response phase during

303    stimulation (Figure 5 A ii, *iii*). We applied this model to examine how the strength of

304    inhibition affects the behavior of simulated afferent fibers with rapid first responses and

305    strong habituation (high gain and low regeneration rates), or slow first responses with no

306    habituation (low gain and high regeneration rates; Figure 5 B *i*). Following from Figure 2,

307    inhibition strength was equal to a 0, 50, or 90% decrease of simulated spontaneous spike

308    rate ($\Delta S$). We then examined the steady evoked spike rate ($\Delta E$) relative to the habituated

309    rate (depicted in Figure 5 A*ii*).

310    　　　　The effects of simulated CD on spike rate differed markedly depending on the

311    level of habituation (Figure 5 B *i*). Inhibition had much less effect on the high-gain

312    (habituating) compared to low-gain (non-habituating) parameter set. The relationship

313    between $\Delta S$ and $\Delta E$ mirrored that observed experimentally (Figure 2 B) in that the level

314    of habituation predicted a divergence in the apparent level of inhibition by CD. We found

315    $\Delta E \ll \Delta S$ in the high-gain parameter set and $\Delta E = \Delta S$ in the low-gain set (Figure 5 B *ii*).

316    The responses were identical at low levels of suppression, regardless of habituation rate,

11

317    which supported the identification of Group 4 highly-habituating but lowly-suppressed

318    cells (Figure 2 B).

319        Finally, we examined how CD affects phase relationships of simulated responses

320    with respect to the peak stimulus. Simulated high gain caused responses that were phase-

321    leading with respect to the stimulus input (peak at $\pi/2$), but became delayed over the

322    course of habituation (Figure 5 B *iii*). Conversely, the low-gain responses exhibited

323    constant phase centered on the peak of the input stimulus, in fact similar to our idealized

324    sensor (Figure 1 Bii). In both parameter sets, moderate inhibition (50%) had minimal

325    effects on spike rate or phase, which might explain why the strength of suppression

326    appears to be bimodally distributed (40). However, strong inhibition (90%) suppressed

327    the tendency of the high-gain parameter set to habituate, as shown by the relative spike

328    rates of Figure 5 Bi). In addition, strong inhibition suppressed the distortion of the

329    median phase by spreading spikes more evenly over the first interval and maintaining

330    constant phase thereafter. The same level of inhibition greatly narrowed response

331    intervals of the non-habituating parameter set. Crucially, high levels of inhibition in both

332    parameter sets resulted in median phase approaching the stimulus peak. We conclude that

333    CD functions to regulate the temporal structure of afferent spikes to achieve constant

334    median phase with zero or minimal delay.

335        In our experimental recordings, the majority of strongly habituating units (Group

336    3 in Figure 2 Bi) were strongly inhibited, as judged by $\Delta S$. Our simulations support

337    labelling the Group3 units as high gain. Strong inhibition by CD will prevent habituation

338    by moderately reducing the signalling interval, and cause their median response phase to

339    converge on $\pi/2$. In contrast, strong inhibition of weakly-habituating units (Group 2,

340    Figure 2 Bi) dramatically reduces their response interval, which remains centered on $\pi/2$.

341    Altogether, we expect that the CD should maintain consistent feedback that can signal the

342    position of the mechanical body wave (Figure 1).

343

**Discussion**

344

345    Axial undulation is the ancestral mode of vertebrate locomotion, predating paired

346 appendages, and is defined by a traveling body wave that enables propulsion through

347 complex environments. To stabilize this mode while navigating, undulating fish must

348 have a sense of self-motion and body position, yet they lack many of the classes and

349 much of the distribution of proprioceptors found in other vertebrates (44, 45). Fish

350 nonetheless possess a complement of proprioceptors which appear to be suited to sensing

351 undulation-associated stresses from the inside out: within the body, on the surface of the

352 body, and at the body-fluid interface. This integrated sensing system is supported by

353 mechanosensors within the spinal cord (46), stretch sensors in the skin (45), and fluid-

354 coupled sensing in the lateral line (24). The role of the lateral line has been the least clear,

355 in large part because an external proprioceptor would fundamentally differ from better-

356 understood mechanisms of actuator- and joint-embedded proprioceptors, like stretch

357 receptors (44). Moreover, the lateral line is not a dedicated proprioceptor, and so it has

358 been uncertain how apparent motion artefacts could be discriminated from environmental

359 stimuli and then transformed to useful proprioceptive feedback. We develop a model

360 based on sensing the alternating flow currents within the undulating body's boundary

361 layer (Figure 1), including a vital role for corollary discharge (CD). We hypothesize that

362 fish robustly detect the peak of neuromast cupular deflection (Figure 1), but that intrinsic

363 sensor heterogeneity will increase response variability to obscure the timing of peak

364 deflection (Figure 1, 3). We find that CD reduces variability while swimming by

365 suppressing habituation (Figure 4) and, through stronger suppression of high-gain cells

366 identified in this paper, homogenizes response phases (Figure 5). By suppressing

367 habituation, the CD maintains robust sensing after the swim bout (Figure 3), when a fish

368 could otherwise experience a period of sensory blindness.

369    Differences in gain can serve as a major source of heterogeneity in lateral line

370 initial and sustained sensitivity (Figures 2, 3). Maintaining populations of cells with large

371 variation in response gain ensures a wide dynamic range for functions like frequency and

372 spatial filtering (21, 22, 47). For instance, high-gain sensors would provide an advantage

13

373    for early sensing of a predator's flow perturbations (48). The wide range in gain may

374    provide sensory advantages for a stationary animal, but would also increase variability in

375    response to self-stimulation and thus complicate the problems of reafference while

376    swimming (Figures 3, 5). Units with greater gain exhibit earlier vesicle release during the

377    stimulus cycle and experience greater habituation, which depletes vesicle pools until they

378    are regenerated. This in turn decreases sensitivity and results in temporal distortions

379    (Figures 3, 5). This is particularly evident in units from response Groups 1, 2, and 3,

380    which have initial gain greater than unity but fall to ≤1 thereafter (Figure 3 Bi). The

381    experimental and computational results identify differences in average phase and changes

382    in phase due to habituation according to gain (Figures 3, 5).

383          The variability in afferent responses caused by self-stimulation during swimming

384    leads us to posit that differential gain modulation through CD is a crucial element of

385    sensorimotor integration. The interaction between level of habituation and CD strength

386    gave rise to four identifiable groups of cells (Figure 2) that were subsequently identified

387    in our simulations as low- and high-gain units with weak or strong suppression (Figure

388    5). Across all cell groups, hair cell hyperpolarization by the CD prevented habituation

389    (Figures 2, 5) and sustained sensitivity throughout the swim bout and after (Figure 4).

390    Simulated respones of low- and high-gain afferent units revealed that strong CD was

391    required to prevent the habituation of the high-gain units. This may explain why nearly

392    all the highly habituating units also had strong inhibition (i.e., those in Group 3, Figure

393    2). A small subset of cells, labelled Group 4, were high gain but with weak inhibition

394    (Figure 2 B, 5 Bii). We were unable to determine each unit's directional preference, but

395    the weak inhibition might suggest rostrocaudal polarization (40). If so, then their high

396    gain notwithstanding, these units would be expected to experience only weak reafference

397    and habituation during forward swimming. In addition to controlling habituation among

398    units with variable gain, the CD also largely homogenizes responses with respect to the

399    stimulus phase, ensuring consistent timing of feedback throughout the swim bout

400    (Figures 4 C, 5 Biii). Importantly, the CD ensures that the response interval is narrow and

401    centered on the peak stimulus phase (Figures 1 B, 5 B *iii*). Interestingly, this implies that

402    the CD synergistically interacts with hair cell polarization to sharpen directional tuning, a

14

403 possibility that had been dismissed on the grounds that the efferent system is not

404 sufficiently specific (25). However, our model shows that the synergy emerges from a

405 hyperpolarization mechanism rather than any degree of efferent specificity.

406 Given that strong suppression was necessary to control habituation in the high-

407 gain units, why might all hair cells not be suppressed as strongly as possible? Our

408 findings support the hypothesis that CD evolved to suppress afferent spiking as much as

409 necessary, but not more (40). One consequence of universally strong CD inhibition would

410 be the elimination of weaker reafference signals from retrograde flows that are relatively

411 weaker during forward swims (40). A second consequence is that strong inhibition would

412 lead to post-swim artefacts. In the absence of stimulation, CD ON caused post-swim

413 rebound spiking (Figure 4), similarly to galvanic stimulation of cholinergic fibers in the

414 auditory system (38). Excessive inhibition causing rebound spiking in the caudal to

415 rostral direction could be misinterpreted as a predator attack from behind. A requirement

416 of the CD is therefore that it be calibrated to control motion artefacts without introducing

417 new ones.

418 We propose that the CD is an essential component of proprioceptive feedback in

419 most fishes. It is, though, conspicuously absent in sea lamprey, a basal jawless fish that

420 have been shown to rely on lateral line proprioception for kinematic control (24).

421 Biofluiddynamic differences between adult lamprey and larval zebrafish notwithstanding,

422 we suggest that the sea lamprey's proprioceptive lateral line can operate without CD

423 because of its low self-stimulation frequency. Typical adult sea lamprey tail beat

424 frequencies lie between ~2-4 Hz (24); at 5 Hz stimulation in zebrafish, we observed

425 minimal habituation but the CD had substantial effects including delayed spike latency

426 and median spike phase (Figure 3 D). At low frequencies, the lateral line therefore

427 behaves similarly to our idealized sensor (Figure 1 Bii), which would suggest that

428 suppression through CD may be deleterious to sensing. In this respect, it is important to

429 consider that hair cells are hyperpolarized for half the stimulus cycle when they are

430 deflected against their preferred direction. This is critical because it not only enables in

431 directional specificity, as is most frequently studied, but it also provides a vesicle

432     regeneration interval *within* the swim cycle and not just after. Indeed, this may be the

433     major reason why we observed little habituation at 5 Hz stimulation, despite the very

434     large number of spikes per stimulus interval (Figure 3A, D). A consequent prediction is

435     that there should be minimal suppression in slow or sedentary species that nonetheless

436     possess a CD, because they will experience minimal habituation. Indeed, the oyster

437     toadfish (*Opsanus tau*) is a teleost that possesses a CD but exhibits very little suppression

438     in spike rates during slow forward swimming (27). This echoes the dynamics that we

439     observed and simulated in the zebrafish lateral line, which is that strong inhibition is

440     principally active in cells with greater propensities for habituation. Altogether, this

441     suggests that the CD is crucial for fast swimmers with higher tail beat frequencies, and

442     that there is a wide evolutionary scope for its strength and role in feedback. Fishes are

443     enormously diverse, so the strength and role of CD in feedback should be studied within

444     their varied ecological and biomechanical contexts.

445        We propose that controlling the effects of habituation is crucial, but we also

446     recognize that some degree of habituation that does not impair sensing can be

447     advantageous. Habituation can enable functions like source localization through bilateral

448     comparisons or other detectors, as occurs in the auditory and electrosensory systems (3,

449     4, 30). In a related manner, habituation could contribute to rheotactic behaviors, in which

450     fish orient upstream by comparing bilateral differences in water velocity, presumably

451     encoded by differences in spike rate (12). Bilateral differences in flow will cause

452     differential habituation, and as a logical extension of our results, bilateral differences in

453     spike timing as well. Temporal information, as well as rate, could therefore be involved

454     in orienting to flows. Overall, the processing of temporal information must occur on real

455     behavioral time scales much shorter than the tens of seconds or even minutes studied in

456     previous lateral line work (20, 49, 50). Exploratory swim bouts of zebrafish larvae last as

457     few as 3-5 tail beats [150-250 ms at 20 Hz, (42)], so reafference and habituation

458     dynamics over a few tail beat cycles represent a substantial portion of the swim.

459     Rheotactic swims last longer, up to 15 tail beats [750 ms at 20 Hz, (51)], so dynamics on

460     a longer time scale are also relevant to sensing capacity during and after sustained

461     behaviors. Our stimulus period of 1 s represents the upper limit of fictive swim durations

16

462     (Supplementary Fig. S2). An essential advance will therefore be to understand the course

463     of hydrodynamic stimulation and CD's inhibition on realistic behavioral time scales,

464     because the strengths of stimulation and inhibition change both during and after swims

465     (25, 35, 37, 41, 42). Time-dependent changes in inhibition strength (41) may control

466     more intense reafferent signals at the swim start that are associated with stronger first

467     tailbeats (42), rostral-caudal flow (40), or the kinetics of the rapid vesicle pool (52).

468     Precisely and faithfully preserving the phase characteristics of a stimulus is a key

469     function of auditory (30). We argue that through the actions of the CD, the lateral line

470     likewise faithfully signals the phase lag between sequential neuromasts to provide

471     proprioceptive feedback of the mechanical body wave during undulatory swimming.

## Materials and Methods
*Electrophysiological recordings*

Adult zebrafish (*Danio rerio*) were obtained from a laboratory-bred population and housed as described previously (e.g., (20, 37, 53), in accordance with protocols approved by the University of Florida's Institutional Animal Care and Use Committee. Protocols were based on our previous study (37). Larvae from 4 to 6 dpf were paralyzed by immersion in 1 mg/mL α-bungarotoxin (Reptile World Serpentarium, St Cloud, Florida) diluted in 10% Hank's extracellular solution (37), and then washed and replaced in extracellular solution until experiments (>30 mins). α-bungarotoxin blockade of the neuronal-type nicotinic acetylcholine receptor (nAChR) α9 found in neuromasts is reversible after a brief washout period (54). Larvae were pinned laterally to a Sylgard-bottomed dish using etched tungsten pins inserted through the dorsal notochord at the anus, at a second location immediately caudal to the yolk sac (approximately at neuromast L1), and through the otic capsule. The preparation was then covered in extracellular solution for recording. Fish health was monitored by blood flow.

We reliably obtained single-unit afferent recordings, or occasionally two clearly differentiable units, using borosilicate glass pipettes with diameters ~15 μm. At this pipette diameter, it was necessary to approach the ganglion under high pressure (–150 to –200mmHg) in order to break in. Once a unit was located, pressure was released sufficiently to maintain a stable recording (typically between 0 and –75 mmHg). In most cases, the afferent recording was stable for hours. Afferent recordings were performed at 20 kHz with 50V/mV gain, Bessel filter of 1 kHz, and an AC high-pass filter of 300 Hz. Signals were amplified through an Axon Instruments CV-7B head stage (MD: Molecular Devices, San Jose, CA) and an Axoclamp 700B amplifier (MD), then recorded with a Digidata 1440A digitizer and pClamp10.7 (MD). Spike times were obtained by thresholding in Clampfit 10.7 (MD). Once an afferent unit was identified, we systematically probed neuromasts for the stereotypical afferent evoked response to a periodic stimulus (20), using a glass bead attached to a single-axis piezo stimulator (30V300, piezosystem jena, Inc., Hopedale, MA). Dipole fluid motions of this type are commonly used to assess near- and far-field responses to oscillatory stimuli, such as from

18

502    prey or conspecifics (12, 48, 55). The dipole vibrating at 20 or 40 Hz simulates

503    neuromast stimulation by the larva's own movements, because reafference *in vivo* is

504    associated with alternating (23, 24) rather than direct currents (40, 41). Stimulation at 5

505    Hz was also performed to compare responses to a frequency at the extreme lower limit of

506    typical tail beats (42). The probe head was roughly spherical with a diameter of 56.6 μm,

507    formed by melting the tip of a recording pipette using a MF-830 microforge (Narishige

508    International, Amityville, NY). Probing started at D1 and continued down the body until

509    the evoked response was elicited. The majority of units could be stimulated by D1 (n=16)

510    or D2 (n=3), and were classified as D-type, and only a few units did not exhibit responses

511    until we reached L1 (n=1), LII.1 or LII.2 (each n=2), or LII.3 (n=1), classified as L-type.

512    In one case we were unable to locate any attached neuromast. Note that, because we only

513    identify the most proximally innervated neuromast, the afferents could have been

514    connected to more distal neuromasts as well (22). After identifying the neuromast, the

515    probe was placed one diameter away from the cupula, and stimulation was performed

516    with a constant ~8 μm amplitude. At no point was the cupula itself touched, which

517    substantially alters responses of the hair cell-afferent group (20).

518            Once an afferent and associated neuromast were identified, we obtained

519    extracellular recordings of the ventral root (VR) arborizations in the myotomal cleft (37).

520    Pressure in the pipette was manually controlled through a syringe. Ventral root

521    recordings were acquired as per afferent units, but with a gain of 100V/mv. Swim bouts

522    were preprocessed by thresholding the VR signal in Clampfit 10.7, and then manually

523    curated using custom software in R 3.6.0 (56). Ventral root recordings were stable for

524    ~15–60 mins. All swims were spontaneous or elicited by a light flash.

525    *Data processing*

526            We recorded 100 sweeps with the stimulus on for 1 s then off for 2 s, which

527    ensured recovery of afferent spike rate in all but one possible case (Figure 3 B). We first

528    examined responses at 20 Hz (*n*=22), then one or both of 40 Hz (*n*=15) or 5 Hz (*n*=13)

529    depending on preparation stability. Additional recordings were performed as required to

530    guarantee sufficient numbers of swims for analysis. Traces were divided into intervals

19

531 according to the presence or absence of a swim or stimulation period (Figure 2). The

532 post-swim interval was equal in duration to the swim (37). Spontaneous spike rates were

533 calculated from periods in which none of these conditions were present. Evoked

534 responses were quantified either as a function of stimulus number or the average over the

535 stimulation period (Figure 2). Within a stimulus interval of period $T$, the phase $\theta$ of a

536 spike occurring at time $t$ was expressed as $\theta = t/T$. The phase can then be used to examine

537 distributional properties of spikes, such as central tendency or width. The commonly

538 reported vector strength (VS, e.g., (20)) for a set of $n$ spikes is calculated by,

$$ \text{VS} = \frac{1}{n}\sqrt{\left(\sum \cos\theta\right)^2 + \left(\sum \sin\theta\right)^2} \qquad \text{eq 2} $$

539 and is related to the circular variance according to $\sigma^2 = -2\log(\text{VS})$ but is constrained to

540 lie within [0,1], with VS→1 as the interval narrows. Single spikes' information content is

541 quantified by the gain, which is calculated by the product of spike count and VS. We

542 additionally computed lower, median, and upper quantiles (0.1, 0.5, and 0.9 quantiles, $q$)

543 of the phases, which reflect the tails of the spike phase distribution while being more

544 robust than the minima (i.e., latency to first spike) and maxima.

545        Spike counts were modelled with a quasi-Poisson distribution, and arcsin-

546 transformed vector strength and the spike phase quantiles were modelled through

547 Gaussian distributions. The intermittent swims resulted in fewer intervals with swims

548 than inactivity, and so less precise estimates of responses during the swim period. For

549 example, an evoked spike might be observed in 85 of $N=95$ ($p=0.89$) stimuli

550 presentations while inactive, but four of $N=5$ ($p=0.80$) presentations while swimming, an

551 apparent decrease in probability during the swim. Uncertainty due to sampling was

552 incorporated through observation weights of $\sqrt{N}/\overline{\sqrt{N}}$. In total, we observed 5859 swims

553 across all individuals and frequencies. Modelled relationships were transformed to the

554 response scale for plotting.

555 *Statistical analysis*

556    Differences due to habituation and swimming were characterized through

557 generalized linear models (GLM). Modelling was performed with the R function *glmer()*,

558 with Tukey post-hoc tests performed with the function *glht()* in package *multcomp* (57).

559 These contrasts were chosen to examine average differences in each condition and to

560 compare our results to literature values (Supplementary Fig. S2). Significant differences

561 in means were assessed by confidence intervals that excluded 0. All models were fit by

562 maximum likelihood. Throughout, we provide relevant estimate effects and 95%

563 confidence intervals; full statistical models (R summaries), including relevant *p*-values,

564 are included in SI Appendix. Statistical significance was tested at $\alpha=0.05$.

565    The relationships between $\Delta S$, $\Delta E$, and habituation were explored through linear

566 models and cluster analysis. The level of habituation was estimated as the difference in

567 responses to the first and last stimulus. We found that directly averaging first and last

568 responses was prone to high variance, likely due to sampling error, and therefore we used

569 a more stable estimate obtained from the predicted response at each stimulus for each

570 individual at each frequency in the population GAM (Figure 3 C, see below). The

571 prediction of $\Delta E$ from $\Delta S$ and habituation was then studied in a linear mixed effects

572 model (R package *nlme*, (58)), with individual nested in frequency. The slope was forced

573 through zero so that the approximate confidence intervals of the predictors could be

574 compared to zero or unity to assess significance. Individual $\Delta S$, $\Delta E$, and habituation

575 responses were clustered using finite Gaussian mixture models (59), and post-hoc

576 analyses of the groups performed to illustrate the magnitude of differences between

577 clusters.

578    We used generalized additive models (GAMs) to model the nonlinear responses

579 over the stimulus period as a non-parametric smooth function (60, 61). We employ an

580 adaptive spline basis set (61) with the upper limit of spline knots respectively set to the

581 frequency, i.e., the number of response intervals. We allow for random variation in the

582 function among identified cell response groups (factor-smooth, (61)), which allows for

583 response heterogeneity among classes (e.g., (21, 22)). A fixed effect of intercept was

584 included, as well as random slopes between stimulus intervals and individual neuron. The

21

585 smooth portion of the fit is centered on zero, so differences in average responses between

586 spikes labelled as occurring during inactivity or swimming are accounted for through

587 parametric intercept differences (inactivity was the reference level). The relative

588 difference in intercepts, expressed as swim intercept/inactivity intercept, is used to model

589 the average change during swims. Arcsin-transformed vector strength was modelled with

590 a Gaussian error distribution, and spike counts and gain were modelled with a quasi-

591 Poisson distribution. Lower quantile ($0.1q$) was cube-transformed prior to analysis to

592 stabilize the variance.

593   The GAM modelling is also appropriate for examining changes in evoked

594 responses during and after the swim. Within each individual at each frequency, we

595 selected swims that fell entirely within (1650 swims) or outside (3348) the stimulus

596 interval, which were then aligned by their terminus and normalized to unit duration. We

597 analyzed responses from the swim start up to one swim duration after the swim end as a

598 function of relative time, using an adaptive spline basis. Differences among stimulus

599 frequencies were included as a fixed effect and a factor smooth frequency allowing for

600 frequency-specific trends (61). A random intercept term was included for individual cells.

601 Spontaneous activity was averaged over time (spike rate) rather than per stimulus period.

602   We sought to compare responses between frequencies. The average differences

603 between CD OFF and ON are parametrized in the model, but the smooth fit modelling

604 habituation is nonparametric. We therefore compare model predicted responses by

605 performing 1000 repeated draws from the posterior distributions of the statistical models

606 of first and last stimulus periods, and of the average CD OFF and ON responses. From

607 these draws, we calculate the predicted average effect of habituation (last-first response)

608 and corollary discharge (CD ON-CD OFF). This process results in means and standard

609 errors of each quantity of interest. We compare the probability that the resulting

610 distributions differ at $\alpha=0.05$.

611 *Time-inhomogeneous Markov chain simulations*

612       We explored potential causal mechanisms of the phase relationships discovered

613    experimentally by simulating different biophysical parameter sets giving rise to strong or

614    weak afferent fiber habituation. Hypothetical vesicle release underlying afferent fiber

615    spiking was modelled as a transition between state 1 (a bound vesicle) and state 2

616    (released vesicle, recorded as a spike). The discrete-time transition matrix is given by,

617

$$\begin{bmatrix} 1 \to 1 & 1 \to 2 \\ 2 \to 1 & 2 \to 2 \end{bmatrix} = \begin{bmatrix} P_A & P_B \\ P_C & P_D \end{bmatrix} = \begin{bmatrix} 1 - P_B & (a \cdot s(t) + d \cdot b)\lambda^* \\ c\lambda^* & 1 - P_C \end{bmatrix}$$

618    The transition matrix elements are normalized to stimulus wavelength divided by

619    sampling frequency ($\lambda^*$, simulated at 1000 Hz). Spontaneous spike rate, $b$, is the number

620    of expected spikes per stimulus wavelength. The magnitude of inhibition is given by the

621    expected suppression of the spontaneous spike rate, $\Delta S$. In the absence of inhibition

622    ($d=1$), a vesicle has non-zero release probability for all $a=0$. The stimulus is modelled by

623    a time-dependent stimulus function, $s(t)$, multiplied by the gain, $a$. When $s(t)$ is constant,

624    a time-invariant stimulus, a rapid burst of evoked spikes rapidly settle into a constant rate

625    that reflects the balance of regeneration and release probabilities. For time-varying

626    stimuli, the responses depend on the relative coefficient magnitudes. The expected

627    regeneration rate per $\lambda^*$ is given by $c$. Habituation can occur when regeneration rates are

628    outpaced by the high probability of release ($a \gg c$). A parameter set for high-probability

629    release vesicles was chosen to qualitatively reflect the readily releasable pool in hair cells

630    and retinal bipolar neurons (29, 62) ($a=0.04$, $b=4$, $c=4$). Conversely, the low-probability

631    parameter set was chosen to minimize habituation through low release rates and high

632    regeneration ($a=4$, $b=40$, $c=0.04$). The lower $b$ in the latter case was chosen to prevent

633    spontaneous spike rates from dominating the evoked responses. The stimulus duration

634    was 20 $\lambda^*$, with $s=0$ for the first half of the period to allow vesicles to regenerate.

635    Inhibition was applied only during the stimulus period, with $d=0$, 0.5, or 0.1 (0, 50, or

636    90% inhibition). Simulations were run for 2-20k iterations as required to depict smooth

637    responses in Figure 5. The first two iterations were discarded as burn-in to avoid impacts

638    of the initialization conditions. We then analyzed averaged responses from each

639    parameter set.

640        Data and modelling code have been deposited in the online repository available at

641    DOI 10.6084/m9.figshare.13034012.


642

**Acknowledgments**
643

644

651

**Competing interests**
652

653    The authors declare that they have no competing interests.

654

## References

1.  T. B. Crapse, M. A. Sommer, Corollary discharge across the animal kingdom. *Nature Reviews Neuroscience* **9**, 587–600 (2008).

2.  F. B. Krasne, J. S. Bryan, Habituation: Regulation through Presynaptic Inhibition. *Science* **182**, 590–592 (1973).

3.  V. Givois, G. S. Pollack, Sensory habituation of auditory receptor neurons: implications for sound localization. *Journal of Experimental Biology* **203**, 2529–2537 (2000).

4.  S. Carver, E. Roth, N. J. Cowan, E. S. Fortune, Synaptic Plasticity Can Produce and Enhance Direction Selectivity. *PLOS Computational Biology* **4**, e32 (2008).

5.  L. Sheets, Excessive activation of ionotropic glutamate receptors induces apoptotic hair-cell death independent of afferent and efferent innervation. *Scientific Reports* **7**, 1–14 (2017).

6.  H. Straka, J. Simmers, B. P. Chagnaud, A New Perspective on Predictive Motor Signaling. *Current Biology* **28**, R232–R243 (2018).

7.  K. T. Sillar, A. Roberts, A neuronal mechanism for sensory gating during locomotion in a vertebrate. *Nature* **331**, 262–265 (1988).

8.  J. F. A. Poulet, B. Hedwig, A corollary discharge maintains auditory sensitivity during sound production. *Nature* **418**, 872–876 (2002).

9.  J. C. Montgomery, D. Bodznick, An adaptive filter that cancels self-induced noise in the electrosensory and lateral line mechanosensory systems of fish. *Neuroscience Letters* **174**, 145–148 (1994).

10. C. C. Bell, An Efference Copy Which is Modified by Reafferent Input. *Science* **214**, 450–453 (1981).

11. D. M. Wolpert, R. C. Miall, M. Kawato, Internal models in the cerebellum. *Trends in Cognitive Sciences* **2**, 338–347 (1998).

12. P. Oteiza, I. Odstrcil, G. Lauder, R. Portugues, F. Engert, A novel mechanism for mechanosensory-based rheotaxis in larval zebrafish. *Nature* **547**, 445–448 (2017).

13. J. Engelmann, W. Hanke, J. Mogdans, H. Bleckmann, Hydrodynamic stimuli and the fish lateral line. *Nature* **408**, 51 (2000).

14. A. B. Kroese, N. A. Schellart, Velocity- and acceleration-sensitive units in the trunk lateral line of the trout. *Journal of Neurophysiology* **68**, 2212–2221 (1992).

15. R. Holzman, S. Perkol-Finkel, G. Zilman, Mexican blind cavefish use mouth suction to detect obstacles. *Journal of Experimental Biology* **217**, 1955–1962 (2014).

16. M. Kulpa, J. Bak-Coleman, S. Coombs, The lateral line is necessary for blind cavefish rheotaxis in non-uniform flow. *Journal of Experimental Biology* **218**, 1603–1612 (2015).

25

689   17.   E. Lloyd, *et al.*, Evolutionary shift towards lateral line dependent prey capture behavior in
690         the blind Mexican cavefish. *Developmental Biology* **441**, 328–337 (2018).

691   18.   T. B. de Perera, Fish Can Encode Order in Their Spatial Map. *Proceedings: Biological
692         Sciences* **271**, 2131–2134 (2004).

693   19.   M. J. McHenry, J. A. Strother, S. M. van Netten, Mechanical filtering by the boundary layer
694         and fluid–structure interaction in the superficial neuromast of the fish lateral line system. *J
695         Comp Physiol A* **194**, 795 (2008).

696   20.   R. Levi, O. Akanyeti, A. Ballo, J. C. Liao, Frequency response properties of primary
697         afferent neurons in the posterior lateral line system of larval zebrafish. *Journal of
698         Neurophysiology* **113**, 657–668 (2014).

699   21.   P. Pichler, L. Lagnado, The Transfer Characteristics of Hair Cells Encoding Mechanical
700         Stimuli in the Lateral Line of Zebrafish. *J. Neurosci.* **39**, 112–124 (2019).

701   22.   J. C. Liao, M. Haehnel, Physiology of afferent neurons in larval zebrafish provides a
702         functional framework for lateral line somatotopy. *Journal of Neurophysiology* **107**, 2615–
703         2623 (2012).

704   23.   B. L. Roberts, Activity of Lateral-Line Sense Organs in Swimming Dogfish. *Journal of
705         Experimental Biology* **56**, 105–118 (1972).

706   24.   A. Ayali, S. Gelman, E. D. Tytell, A. H. Cohen, Lateral-line activity during undulatory
707         body motions suggests a feedback link in closed-loop control of sea lamprey swimming.
708         *Can. J. Zool.* **87**, 671–683 (2009).

709   25.   B. L. Roberts, I. J. Russell, The Activity of Lateral-Line Efferent Neurones in Stationary
710         and Swimming Dogfish. *Journal of Experimental Biology* **57**, 435–448 (1972).

711   26.   J. C. Liao, The role of the lateral line and vision on body kinematics and hydrodynamic
712         preference of rainbow trout in turbulent flow. *Journal of Experimental Biology* **209**, 4077–
713         4090 (2006).

714   27.   A. F. Mensinger, J. C. V. Wert, L. S. Rogers, Lateral line sensitivity in free-swimming
715         toadfish Opsanus tau. *Journal of Experimental Biology* **222**, jeb190587 (2019).

716   28.   S. M. van Netten, T. Dinklo, W. Marcotti, C. J. Kros, Channel gating forces govern
717         accuracy of mechano-electrical transduction in hair cells. *PNAS* **100**, 15510–15515 (2003).

718   29.   J. D. Goutman, E. Glowatzki, Time course and calcium dependence of transmitter release at
719         a single ribbon synapse. *PNAS* **104**, 16341–16346 (2007).

720   30.   D. Pérez-González, M. S. Malmierca, Adaptation in the auditory system: an overview.
721         *Front. Integr. Neurosci.* **8** (2014).

722   31.   B. P. Chagnaud, S. Coombs, "Information Encoding and Processing by the Peripheral
723         Lateral Line System" in *The Lateral Line System*, Springer Handbook of Auditory

724  Research., S. Coombs, H. Bleckmann, R. R. Fay, A. N. Popper, Eds. (Springer New York,
725  2014), pp. 151–194.

726  32.  L. Sheets, *et al.*, Enlargement of Ribbons in Zebrafish Hair Cells Increases Calcium
727        Currents But Disrupts Afferent Spontaneous Activity and Timing of Stimulus Onset. *The*
728        *Journal of Neuroscience* **37**, 6299–6313 (2017).

729  33.  T. Furukawa, S. Matsuura, Adaptive rundown of excitatory post-synaptic potentials at
730        synapses between hair cells and eight nerve fibres in the goldfish. *The Journal of*
731        *Physiology* **276**, 193–209 (1978).

732  34.  A. Faucherre, J. Pujol-Martí, K. Kawakami, H. López-Schier, Afferent Neurons of the
733        Zebrafish Lateral Line Are Strict Selectors of Hair-Cell Orientation. *PLOS ONE* **4**, e4477
734        (2009).

735  35.  Å. Flock, I. J. Russell, The post-synaptic action of efferent fibres in the lateral line organ of
736        the burbot Lota lota. *The Journal of Physiology* **235**, 591–605 (1973).

737  36.  I. Marcovich, *et al.*, Distinct evolutionary trajectories of neuronal and hair cell nicotinic
738        acetylcholine receptors. *bioRxiv*, 621342 (2019).

739  37.  E. T. Lunsford, D. A. Skandalis, J. C. Liao, Efferent modulation of spontaneous lateral line
740        activity during and after zebrafish motor commands. *Journal of Neurophysiology* **122**,
741        2438–2448 (2019).

742  38.  M. J. Moglie, P. A. Fuchs, A. B. Elgoyhen, J. D. Goutman, Compartmentalization of
743        antagonistic Ca2+ signals in developing cochlear hair cells. *PNAS* **115**, E2095–E2104
744        (2018).

745  39.  A. Flock, I. Russell, Inhibition by efferent nerve fibres: action on hair cells and afferent
746        synaptic transmission in the lateral line canal organ of the burbot Lota lota. *The Journal of*
747        *Physiology* **257**, 45–62 (1976).

748  40.  P. Pichler, L. Lagnado, Motor Behavior Selectively Inhibits Hair Cells Activated by
749        Forward Motion in the Lateral Line of Zebrafish. *Current Biology*, S0960982219314599
750        (2019).

751  41.  B. P. Chagnaud, R. Banchi, J. Simmers, H. Straka, Spinal corollary discharge modulates
752        motion sensing during vertebrate locomotion. *Nature Communications* **6**, 7982 (2015).

753  42.  O. Mirat, J. R. Sternberg, K. E. Severi, C. Wyart, ZebraZoom: an automated program for
754        high-throughput behavioral analysis and categorization. *Front. Neural Circuits* **7** (2013).

755  43.  I. J. Russell, The Role of the Lateral-Line Efferent System in Xenopus Laevis. *Journal of*
756        *Experimental Biology* **54**, 621–641 (1971).

757  44.  B. R. Aiello, A. R. Hardy, M. W. Westneat, M. E. Hale, Fins as Mechanosensors for
758        Movement and Touch-Related Behaviors. *Integr Comp Biol* **58**, 844–859 (2018).

759  45.  B. L. Roberts, The response of a proprioceptor to the undulatory movements of dogfish. *Journal of Experimental Biology* **51**, 775–785 (1969).

761  46.  U. L. Böhm, *et al.*, CSF-contacting neurons regulate locomotion by relaying mechanical stimuli to spinal circuits. *Nature Communications* **7**, 10866 (2016).

763  47.  W. J. V. Trump, M. J. McHenry, The morphology and mechanical sensitivity of lateral line receptors in zebrafish larvae (Danio rerio). *Journal of Experimental Biology* **211**, 2105–2115 (2008).

766  48.  W. J. Stewart, A. Nair, H. Jiang, M. J. McHenry, Prey fish escape by sensing the bow wave of a predator. *Journal of Experimental Biology* **217**, 4328–4336 (2014).

768  49.  J. G. Trapani, N. Obholzer, W. Mo, S. E. Brockerhoff, T. Nicolson, synaptojanin1 Is Required for Temporal Fidelity of Synaptic Transmission in Hair Cells. *PLOS Genetics* **5**, e1000480 (2009).

771  50.  C. Lv, *et al.*, Synaptic Ribbons Require Ribeye for Electron Density, Proper Synaptic Localization, and Recruitment of Calcium Channels. *Cell Reports* **15**, 2784–2795 (2016).

773  51.  R. Olive, *et al.*, Rheotaxis of Larval Zebrafish: Behavioral Study of a Multi-Sensory Process. *Front. Syst. Neurosci.* **10** (2016).

775  52.  J. D. Goutman, Mechanisms of synaptic depression at the hair cell ribbon synapse that support auditory nerve function. *PNAS* **114**, 9719–9724 (2017).

777  53.  M. Haehnel, M. Taguchi, J. C. Liao, Heterogeneity and dynamics of lateral line afferent innervation during development in zebrafish (Danio rerio). *Journal of Comparative Neurology* **520**, 1376–1386 (2012).

780  54.  L. A. Poppi, J. C. Holt, R. Lim, A. M. Brichta, A review of efferent cholinergic synaptic transmission in the vestibular periphery and its functional implications. *Journal of Neurophysiology* **123**, 608–629 (2020).

783  55.  K. E. Feitl, V. Ngo, M. J. McHenry, Are fish less responsive to a flow stimulus when swimming? *Journal of Experimental Biology* **213**, 3131–3137 (2010).

785  56.  R Core Team, *R: A Language and Environment for Statistical Computing* (R Foundation for Statistical Computing, 2019).

787  57.  T. Hothorn, F. Bretz, P. Westfall, Simultaneous Inference in General Parametric Models. *Biometrical Journal* **50**, 346–363 (2008).

789  58.  J. C. Pinheiro, D. Bates, S. DebRoy, D. Sarkar, R Core Team, *nlme: Linear and Nonlinear Mixed Effects Models* (2016).

791  59.  L. Scrucca, M. Fop, T. Murphy, A. Raftery, mclust 5: clustering, classification and density estimation using Gaussian finite mixture models. *The R Journal* **8**, 289–317 (2016).

793   60.   N. L. Rose, H. Yang, S. D. Turner, G. L. Simpson, An assessment of the mechanisms for
794          the transfer of lead and mercury from atmospherically contaminated organic soils to lake
795          sediments with particular reference to Scotland, UK. *Geochimica et Cosmochimica Acta* **82**,
796          113–135 (2012).

797   61.   S. N. Wood, *Generalized Additive Models: An Introduction with R, Second Edition*, 2nd Ed.
798          (CRC Press, 2017) (June 18, 2019).

799   62.   H. von Gersdorff, G. Matthews, Depletion and Replenishment of Vesicle Pools at a Ribbon-
800          Type Synaptic Terminal. *J. Neurosci.* **17**, 1919–1927 (1997).

801
802

803



804
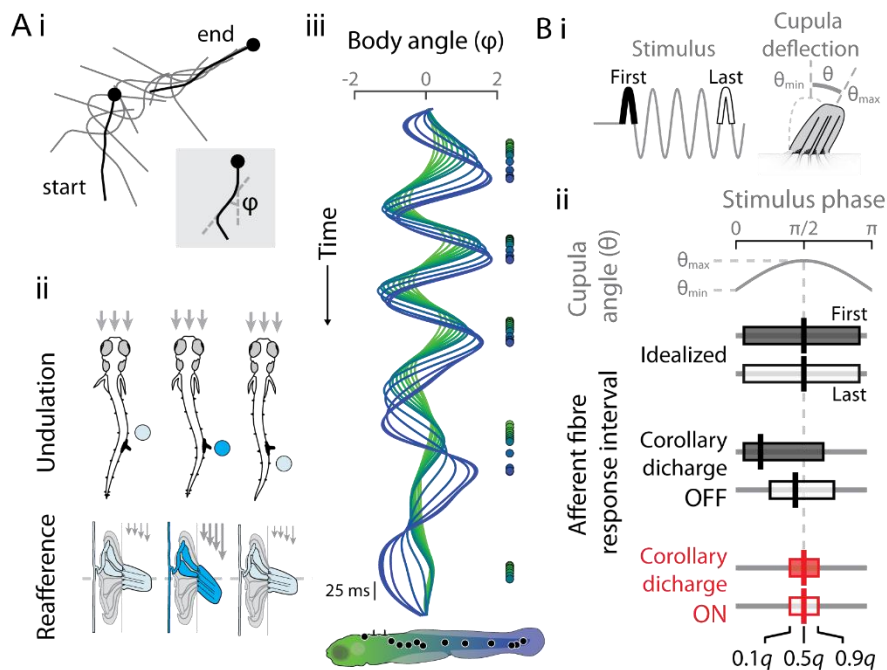
**Figure 1. Timing of lateral line reafference during undulatory locomotion.**

(A) *i* Larval zebrafish swimming is characterized by body undulations. Body midline angles with respect to the head ($\phi$) were determined by a spline from head (ball) to tail. *ii* Undulation involves a mechanical body wave that self-stimulates lateral line neuromasts embedded in the skin. Maximum cupular deflection and reafference (circles colored by reafferent intensity) are predicted to occur as the body wave peak passes the neuromast. *iii* Encoding peak timing allows the lateral line to signal the progression of the body wave by the phase lag between neuromast positions (green-blue color coding along body axis).

(B) *i* Positional proprioception depends on faithful signalling of the maximum cupular deflection timing during repeated stimulation. *ii* An idealized sensor exhibits invariant responses that transduce deflection in the interval $\theta_{min} < \theta \leq \theta_{max}$, such that peak responses coincide with the peak deflection phase, $\pi/2$. When the corollary discharge is OFF, habituation is predicted to cause phase-advanced responses with temporal distortions from the first to last stimulus presentation. Conversely, when corollary discharge is ON we predict that habituation is suppressed, and response intervals will be narrower, constant, and centered on $\pi/2$. In this way, gain modulation by the corollary discharge, together with the phase lag inherent to undulation, may enable positional proprioception through reafferent signalling in the lateral line system of fishes.

823

824



825
826
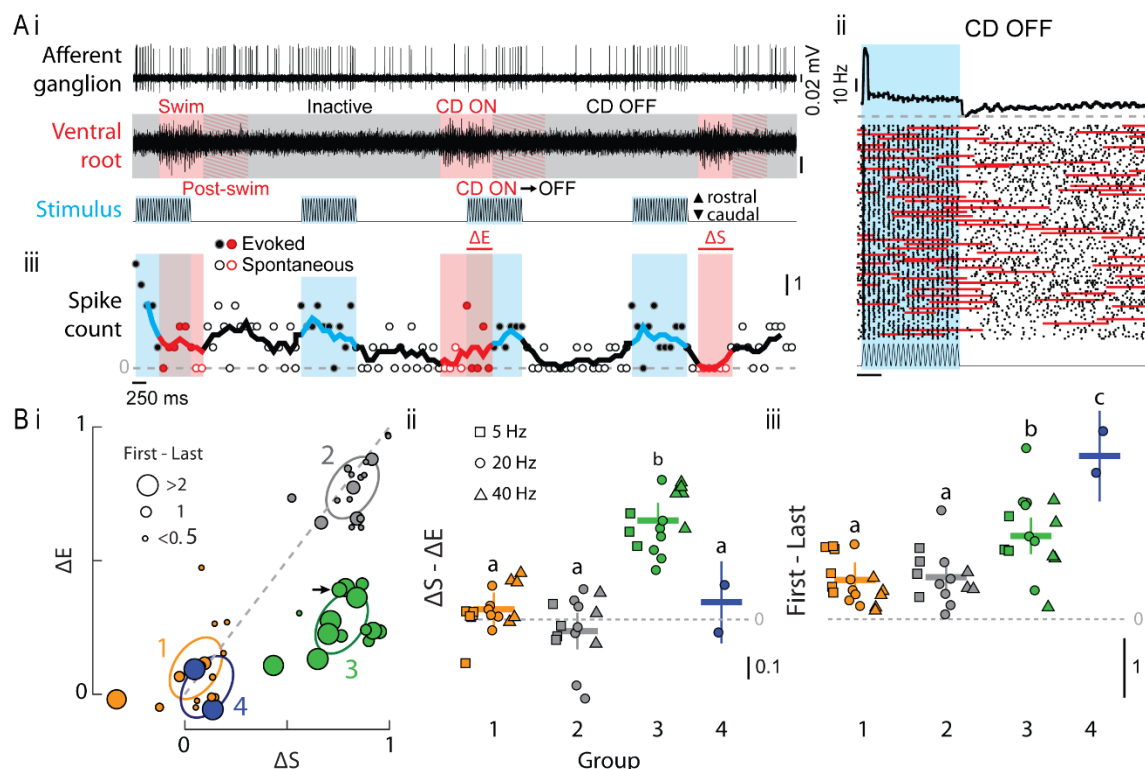
**Figure 2. Afferent neuron spike activity in response to neuromast deflection during and between swims reveals interactions between habituation and corollary discharge (CD).**

(A) *i* Spontaneous and evoked lateral line afferent fiber activity during swim bouts (ventral motor root). Periods of swimming are highlighted in red, and periods of external stimulation of a single neuromast are highlighted in blue. Three periods were distinguished from ventral root recordings, corresponding to the activation of the CD: swim (CD ON), inactivity (CD OFF), and the post-swim transition between the two (CD ON→OFF). *ii* Peristimulus time histogram demonstrating spike rate (spike count per 100 ms) habituation when CD OFF, including decreased spike count and a post-stimulus refractory period. *iii* The impact of swim bouts (CD ON) on spontaneous (open face) and evoked (closed face) responses were analyzed within highlighted intervals. In this trace, the relative decrease in spontaneous spike rate ($\Delta$S) was greater than that of the evoked spike rate ($\Delta$E). There was an immediate restoration of evoked spike activity after the swim bout ended.

(B) *i* Correlation of $\Delta$S and $\Delta$E reveals distinct groups of afferent responses at all frequencies (0=no suppression, 1=complete suppression) that depends on the level of habituation (First – Last spike count). Arrow highlights record corresponding to the trace in A. *ii-iii* Response groups were identified by cluster analysis of $\Delta$S, $\Delta$E, and level of habituation. Post-hoc comparisons among groups show inequality of $\Delta$S and $\Delta$E (*ii*) and

31

849     degree of habituation (*iii*). 5 Hz: n=13 afferent neurons from N=12 individuals; 20 Hz: n
850     = 22, N=21; 40 Hz: n=15, N=14.
851

852



853
854
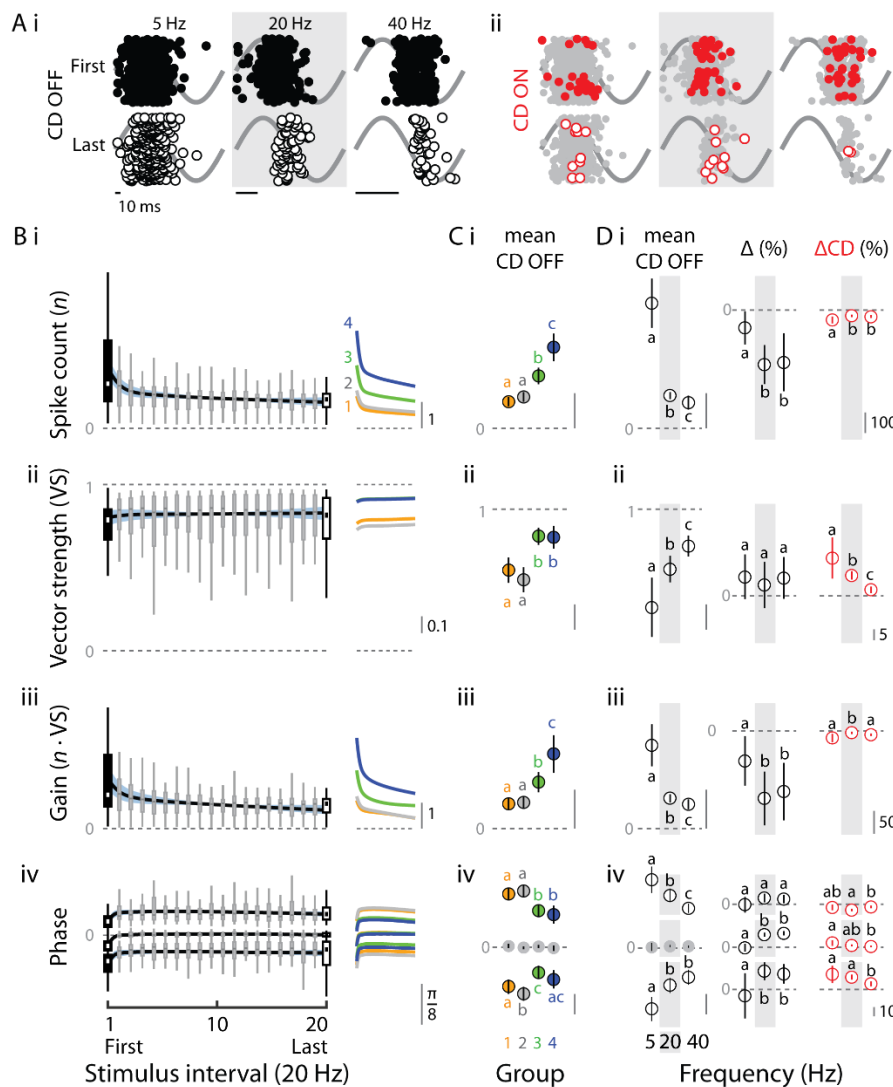
**Figure 3. Effects of habituation and corollary discharge (CD) on evoked afferent fiber spike responses.**

(A) PSTH of spike phases (circles overlaid on sinusoidal stimulus) grouped by the first (solid symbols) and last (open face) stimulus period and by CD OFF (*i*) or CD ON (*ii*). *i* At all frequencies, CD OFF results in habituation and significantly delayed response intervals. *ii* CD ON reduces spike number and causes narrowed and shifted responses intervals with respect to CD OFF (shaded for comparison). Data for individual in Figure 2 A.

(B) Box-and-whisker plots of stimulus-averaged spike count, vector strength, gain, and response phase at 20 Hz. The average time-dependent changes between first and last intervals during CD OFF were quantified by smooth functions. *Right*: Time courses of responses for response groups identified in Figure 2.

33

869

870 (C) Mean responses among groups. Group 1 and 2 cell responses were not statistically
871 distinguishable, and included lower mean evoked spike rates, vector strength, and gain
872 compared to Group 3 and 4 cells. Note that median phase cannot be analyzed, as
873 described in the text.

874

875 (D) Frequency-dependence of mean responses, habituation, and CD ON. Higher
876 stimulation frequencies resulted in reduced spike counts, higher vector strength, and
877 lower gain. Narrower response intervals coincide with the change in vector strength. The
878 relative effects of habituation. The relative impact of habituation ($\Delta\%$) on spike count
879 and gain was lower at 5 Hz compared to 20 and 40 Hz, whereas the relative effect of CD
880 ($\Delta CD\%$) was relatively greater. Across frequencies, there was an equal but nonsignificant
881 overall increase in vector strength with habituation, whereas the relative effect of CD
882 decreased with higher frequencies. There was no observable effect of habituation to the 5
883 Hz stimulus on spike phase, but CD caused a relatively large delay of the earliest spikes
884 and relatively small advance of the late spikes, resulting in later median phases. These
885 effects diminished at higher frequencies, reducing the change in median phase.

886

887 Sample sizes as in Figure 1. $p < 0.001$ for depicted smooth functions in all panels. All
888 effects in C and D are means and standard errors.

889
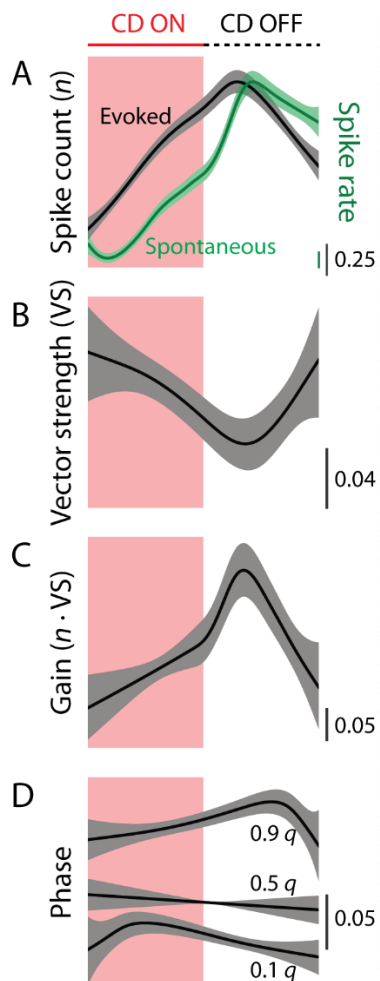
**Figure 4. Corollary discharge counteracts habituation and preserves sensitivity after swimming**.

Swim bouts and a subsequent post-swim period of equal time were normalized to unit duration. These periods correspond to CD ON (swimming, red) followed by CD OFF (white), although residual effects of CD ON persist into the post-swim period (37). All effects normalised to start of trace.

(A) Spontaneous (green) and evoked (black) spike counts were maximal in the post-swim period. The rise in evoked spike count with CD ON contrasts to the fall in responses with CD OFF (see Figures 2 Aii, 3 B). Significance of smooth functions, $p<0.001$.

(B) Vector strength was initially high, representing a narrow response interval, and exhibited a post-swim minimum ($p<0.001$).

(C) Afferent signal gain reached a maximum during the post-swim period ($p<0.001$). There appears to be an inflection point toward increased gain corresponding to the end of

909    CD ON.

910

911    (D) The response interval width is narrower during CD ON, as as indicated by a smaller

912    separation between $0.1q$ and $0.9q$. During CD ON, $0.1q$ is significantly delayed (rising

913    trend) but becomes advanced (falling trend) through the swim and CD OFF periods ($0.1q$:

914    $p=0.02$; $0.9q$: $p=0.04$). In contrast, 0.9q becomes progressively delayed to a peak in the

915    CD OFF period, but then substantially advances. This suggests that response intervals are

916    narrow during CD ON but widen with CD OFF. A relatively constant median response

917    phase ($0.5q$, $p=0.33$) was preserved throughout the CD ON and OFF intervals.

918

919



920
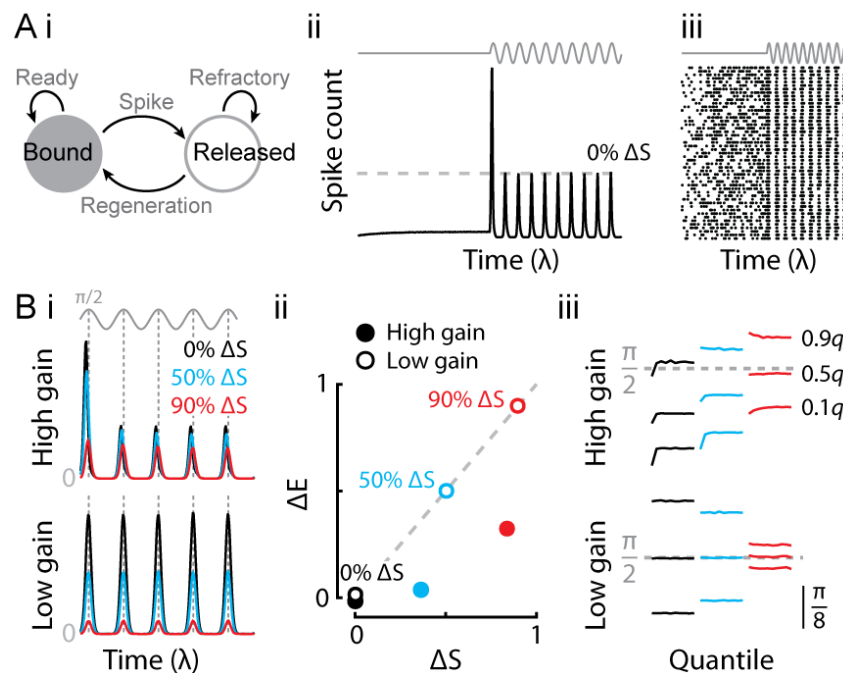
**Figure 5. Corollary discharge counteract habituation to increase proprioceptive information content of afferent signals.**

(A) *i* The relationship of afferent fiber spike phase to the peak of reafference was examined through a state transition model reflecting simple vesicle dynamics. Simulated vesicles may be bound and ready for release, or they may transition to a released state (a spike) and become unavailable until regenerated (transition back to the bound state). *ii* Average responses of a simulated fiber without suppression (0% ΔS) demonstrate major features of experimental recordings including strong initial and subsequently weaker responses, and a distinct refractory period after stimulation. The average habituated level is taken as the reference level for further comparisons (dashed line). *iii* PSTH of responses in *ii* showing variable spike timing within individual stimulus presentations.

(B) *i* Differential effects of corollary discharge on simulated afferent fiber responses. Vertical dashed lines denote the stimulus peak timing at $\pi/2$. We simulated the effects of inhibition equal to 0, 50, or 90% ΔS, on an afferent fiber with strong habituation (high gain) or without (low gain). *ii* Correlation of simulated ΔS and ΔE reveals divergent effects of suppression on high- and low-gain parameter sets. Points at the origin are staggered for clarity. *iii* The high-gain kinetics exhibited time-dependent phase-leading behavior, whereas the low gain kinetics had constant response intervals centered on the stimulus peak at $\pi/2$. When the high-gain kinetics were strongly inhibited (90%), the median response phase converged on the stimulus peak at $\pi/2$, without time-dependent distortions.